Inst. Phys. Conf. Ser. No 102: Session 6a
Paper presented at Int. Conf. Mech. Prop. Materials at High Rates of Strain, Oxford, 1989

Localization analysis under dynamic loading

Y. Leroy†, and M. Ortiz
Division of Engineering, Brown University, Providence, RI 02912

ABSTRACT: A finite element method proposed by Ortiz *et al.* (1987) is used to study shear band formation in rate dependent and rate independent pressure sensitive solids under dynamic loading. Under these conditions, shear bands are observed to propagate in an irregular fashion in time and space. In particular, the development of multiple shear bands appears to be a prevalent mechanism of deformation at sufficiently high impact velocities.

1. Introduction.

Localization of deformation into bands of intense shearing occurs in a wide variety of solids: ductile single crystals, Chang and Asaro (1981), polycrystalline structural metals, Marchand and Duffy (1988), saturated clays, Vardoulakis (1979), rocks, Waversik and Brace (1971) and concrete, van Mier (1984). Localization processes furnish a mechanism for the local accumulation of large plastic deformations, and may be a precursor to ductile shear failure, Marchand and Duffy (1988). The overall response of a solid is sharply influenced by the emerging shear bands. A case in point is the structural softening of sand specimens in plane strain biaxial compression, where the apparent loss of bearing capacity of the sample is a direct consequence of shear banding, Leroy and Ortiz (1989a).

The physical mechanisms which trigger localization vary widely between materials and loading conditions. For example, in structural metals at high rates of loading shear banding is largely governed by two competing mechanisms: thermal softening and rate sensitivity, Marchand and Duffy (1988), the latter having a stabilizing effect, Molinari and Clifton (1987). Localization can also occur in metals at low loading rates. Here, a critical feature of the constitutive response is the presence of vertices in the yield surface, Rice (1976).

Analytical tools for the study of shear bands are presently limited to material instability analyses, Rice (1976), to determine the local conditions for the inception of localization, and to infinite band models, Marciniak and Kuczynski (1967), Hutchinson and Tvergaard (1981). The detailed analysis of more complicated geometries requires the use of numerical techniques. However, conventional isoparametric finite elements can only accommodate the steep strain gradients, discontinuities or shocks associated with the development of localized deformation along the element boundaries. The source of this limitation can be traced to the smooth interpolation which characterizes isoparametric elements. Prompted by these difficulties, several finite element methods have been proposed in recent years (e. g., Tvergaard *et al.*, 1981; Ortiz *et al.*, 1987; Leroy *et al.*, 1988; Belytschko *et al.*, 1988) which facilitate the analysis of strain localization under complex conditions.

Whereas the literature on quasi-static localization is presently quite extensive, there is a paucity of results on dynamic shear banding under multiaxial loading conditions. One of the few analyses available to date was carried out by Freund *et al.* (1985), who considered an hyperelastic solid deforming in anti-plane shear. Freund *et al.* concluded that discontinuous propagation of the band front in a crack-like fashion is possible. More recently, Needleman (1989) analyzed the case of a finitely deforming plastic material undergoing plane strain deformations. A noteworthy outcome of the analysis is the surprisingly

† Presently at Koninklijke/Shell Exploratie en Produktie Laboratorium, The Netherlands

small variation that is observed in the qualitative behavior of shear bands under dynamic and quasi-static loading.

In this paper, we study the localization behavior of pressure sensitive solids subjected to dynamic loading. It is well-known that, under static conditions, lack of normality in the plastic flow may promote localization before maximum load, Mandel (1964), Rudnicki and Rice (1975). For quasi-static loading, the post-bifurcation regime has been analyzed numerically by de Borst (1988) and Leroy and Ortiz (1989a). Here, we focus our investigation on the effect of inertia and rate sensitivity on the initiation and propagation of shear bands. Noteworthy differences with the static case are found to be the appearance of multiple shear bands, the discontinuous stick-slip propagation of the bands, and the unsteadiness of the propagation direction.

2. Localization conditions.

In this section, we review some results concerning localization criteria for rate independent and rate dependent materials. These conditions are pertinent to the formulation of the finite element method proposed by Ortiz *et al.* (1987), as well as to the design of crossed triangular meshes. We restrict our discussion to the case of infinitesimal deformations.

2.1. Localization in rate independent materials.

Consider a rate independent solid obeying rate constitutive equations of the form:

$$\begin{aligned} \dot{\sigma}_{ij} &= D^e_{ijkl}(\dot{\epsilon}_{kl} - \dot{\epsilon}^p_{kl}) \\ \dot{\epsilon}^p_{ij} &= \dot{\gamma} r_{ij}(\sigma, q) \\ \dot{q}_\alpha &= \dot{\gamma} h_\alpha(\sigma, q) \\ \phi(\sigma, q) &= 0 \end{aligned} \tag{1}$$

where σ_{ij} are the stresses acting on the solid, ϵ_{ij} are the current strains, ϵ^p_{ij} the plastic deformations, q_α some suitable set of internal variables, D^e_{ijkl} the elastic moduli, r_{ij} the direction of plastic flow, h_α the hardening moduli, γ an effective plastic strain, and ϕ the yield function. In (1) and henceforth, a superimposed dot is used to signify differentiation with respect to time. Standard manipulations enable one to reduce (1) to the form:

$$\dot{\sigma}_{ij} = D^{ep}_{ijkl}\dot{\epsilon}_{kl} \tag{2}$$

where D^{ep}_{ijkl} are the elastic-plastic moduli.

Next, we seek to determine under which conditions a strain discontinuity, or shock, can arise as a result of a local material instability. For a rate independent solid undergoing quasi-static deformations, this bifurcation is associated with the loss of ellipticity of the governing equations, whereas under dynamic conditions the equations of motion loose hyperbolicity and the wave speeds become imaginary, Hadamard (1903), Thomas(1961), Hill(1962). The Maxwell jump conditions for the velocity gradients $\dot{u}_{i,j}$ across a surface of discontinuity of normal n_i require that

$$[\![\dot{u}_{i,j}]\!] = \dot{g}_i n_j \tag{3}$$

where g_i is a polarization vector for the shock. The jump operator $[\![\cdot]\!]$ gives the difference in the values of a function on the plus and minus sides of the surface of discontinuity. Conservation of linear momentum across a surface traveling at a velocity V relative to the solid requires

$$[\sigma_{ij}]n_j + \rho V[\dot{u}_i] = 0 \tag{4}$$

where ρ is the mass density of the solid. In the case of a stationary discontinuity, $V = 0$, i. e., a material surface following the deformation of the solid, the inertia term drops out from (4).

Following Hill (1958), we now assume that, at the point of inception of localization, the material follows the plastic branch of $\mathbf{D}^{ep}$ on both sides of the emerging surface of discontinuity. This corresponds to considering Hill's linear comparison solid (1958). For solids obeying normality, this criterion is known to provide the earliest bifurcation point. In solids exhibiting moderate deviations from normality, Tvergaard (1982) has found that Hill's linear comparison solid criterion retains its usefulness for approximating the lowest bifurcation point.

Combining eqs. (2), (3) and (4), it is found that non-trivial solutions for the polarization vector are possible only if

$$det(A_{jl}(\mathbf{n})) = det(n_i D^{ep}_{ijkl} n_k) = 0 \tag{5}$$

where $\mathbf{A}$ is the acoustic tensor.

Eq. (5) establishes a necessary condition for the development of a strain discontinuity across a surface of orientation $\mathbf{n}$. Interestingly, the same condition applies to dynamic and quasi-static deformations. The satisfaction of condition (5) implies the vanishing of the discriminant of the equilibrium equations. Thus, condition (5) is associated with a change of type of the governing equations. In the static case, the equations loose ellipticity and the vector $\mathbf{n}$ determines the emerging characteristic directions.

For rate independent solids undergoing adiabatic deformations, the thickness of the band cannot be determined from the field equations, which lack a characteristic dimension. For dynamic loading of rate dependent solids, by contrast, Needleman (1988) has shown that the elastic wave speeds coupled with the characteristic relaxation time of the material set a length scale for the deformation. It should also be noted that, as pointed out by Needleman (1988), the governing equations for rate dependent solids of the viscoplastic type never loose ellipticity and, consequently, the solution is unique. In addition, owing to the ellipticity of the governing equations, defects set a length scale for the solution. These two cases, which constitute the main focus of the work reported here, provide two examples of problems with well-defined characteristic lengths in which the constitutive response is taken to be that of a local or simple continuum. Another physically motivated example is furnished by thermal softening coupled with heat conduction (Molinari and Clifton, 1987). In all of these cases, numerical solutions are free of spurious mesh size dependencies, provided that the appropriate length scales are adequately resolved by the mesh.

As an alternative possibility, other authors have sought to build a length scale directly into the mechanical response by recourse to nonlocal models (Schreyer and Chen, 1984; Frantziskonis and Desai, 1987a, 1987b; Pijaudier-Cabot and Bazant, 1987; Bazant and Pijaudier-Cabot, 1988), and to generalized continuum theories (Triantafyllidis and Aifantis, 1986; Aifantis, 1987, Mühlhaus and Vardoulakis, 1987; Zbib and Aifantis, 1988).

2.2. Localization in rate dependent materials.

Consider the class of rate dependent solids obtained by replacing the yield condition (1c) by a viscosity law of the type

$$\dot{\gamma} = \frac{\phi(\sigma, q)}{\eta} \tag{6}$$

where ϕ may be chosen with dimensions of stress and η is a viscosity parameter. The rate independent limit (1c) is recovered by letting $\eta \to 0$. When rate dependence of the plastic flow is accounted for, there is no loss of ellipticity in quasi-static problems and wave speeds remain real. Localization phenomena are also found in rate dependent solids, however, but in the form of unstable growth of shearing modes of deformation.

Using a linearized instability analysis, Molinari (1988) and Leroy and Ortiz (1989b) have determined necessary conditions for the earliest possible localization instabilities. The essence of the analysis can be outlined as follows. Consider a small perturbation in the displacement field of the form

$$\delta u_i(\mathbf{x},t) = \delta \hat{u}_i(\mathbf{x}) \exp(\lambda t) \tag{7}$$

Then, we seek to ascertain under what conditions this perturbation can grow exponentially in time. Start by writing the corresponding variation in stress and strain as

$$\begin{aligned} \delta\sigma_{ij}(\mathbf{x},t) &= \delta\hat{\sigma}_{ij}(\mathbf{x}) \exp(\lambda t) \\ \delta\epsilon_{ij}(\mathbf{x},t) &= \delta\hat{\epsilon}_{ij}(\mathbf{x}) \exp(\lambda t) \end{aligned} \tag{8}$$

For perturbations of this type, it may be shown (Leroy and Ortiz, 1989b) that the linearized constitutive equations for a rate dependent elastoplastic solid are of the form

$$\delta\hat{\sigma}_{ij} = L_{ijkl}(\lambda)\delta\hat{\epsilon}_{kl} \tag{9}$$

for some moduli L_{ijkl}. Next, specialize the perturbation (7) to a form appropriate for a localization instability,

$$\begin{aligned} \delta\hat{u}_i(\mathbf{x}) &= U(x_n)m_i \\ x_n &= (x_i - x_i^*)n_i \end{aligned} \tag{10}$$

where x_i^* is some reference point on the band, n_i is the unit normal to the band, m_i a unit polarization vector, x_n the coordinate normal to the band, and the function $U(x_n)$ defines the normal profile of the perturbation. Inserting the strains corresponding to (10) into (9) and establising the equilibrium of the resulting stress field, one arrives at the condition

$$det\big(L_{ijkl}(\lambda)n_in_l\big) = 0 \tag{11}$$

If, for a given reference state, a direction n_i can be found for which the corresponding λ following from (11) is positive, we conclude that localization in the form of a band of orientation n_i is possible. The value of λ then gives the rate of growth of the perturbation, and the polarization vector m_i follows as the null eigenvector of the pseudo-acoustic tensor $L_{ijkl}(\lambda)n_in_l$.

Of primary interest in applications is the limiting case of $\lambda \to 0$, which corresponds to perturbations growing at an arbitrarily small rate. Leroy and Ortiz (1989b) have shown that

$$\lim_{\lambda\to 0+} L_{ijkl}(\lambda) = D^{ep}_{ijkl} \tag{12}$$

where D^{ep}_{ijkl} are the rate independent elastoplastic moduli introduced in Section 2.1.

Thus, in the limit $\lambda \to 0$ the localization condition (11) reduces to its rate independent counterpart (5). The boundary between stable and unstable behavior precisely corresponds to conditions for which perturbations can grow at a vanishing rate. Hence, the rate independent limit of the constitutive equations determines the earliest possible time at which localization may take place.

It should be noted that a linearized stability analysis generally provides a necessary but not a sufficient condition for localization. In particular boundary value problems, the progression of localization may be stabilized by nonlinear effects not taken into account in the linearized analysis. As a result, the

actual growth of the localized mode may be delayed relative to the theoretical inception time (Molinari and Clifton, 1987). However, as we shall see, for the purpose of setting up finite element schemes the earliest possible time of localization as determined by the linearized instability analysis is of primary interest.

3. Finite Element Methods.

The response of conventional isoparametric elements can be overly stiff in problems involving strain localization. Finite element analyses of shear banding based on fine meshes of quadrilateral elements built up from four 'crossed' constant strain triangles have given sharply localized modes (see, e.g., Tvergaard *et al.* (1981), Tvergaard, 1982, and the review of Needleman and Tvergaard, 1982). However, the crossed triangle finite element formulation is specifically geared to two dimensional problems, it requires careful mesh design to account for the likely directions of localization and the results are sensitive to the orientation of the mesh relative to the shear band.

More recently, Ortiz, Leroy and Needleman (1987), have proposed a method in which a deformation mode carrying a suitable strain discontinuity is added to the element. The geometry of the localized mode is determined by means of a material stability analysis of the type discussed in Section 2. The amplitudes of the localized modes are eliminated at the element level by static condensation. An extension of the method to finite deformations and rate dependent behavior has been given by Nacar *et al.* (1989). Applications of the method to soils have been pursued by Leroy and Ortiz (1989a).

In all of the above methods, the minimum band thickness is set by the mesh size. Belytschko et al. (1988) have proposed a method which endeavors to endow the elements with sub-mesh size shear band modes. Leroy et al. (1988) have shown that the method of Belytschko et al. (1988) is equivalent to modifying the element constitutive description in a manner which makes the material softer in the direction of localization. The thickness of the softened region, however, is still bounded below by the mesh size.

4. Numerical examples

Our first example is intended to illustrate the finite element method used in subsequent analyses. The problem concerns a single four noded element deforming quasi-statically in plane strain under an applied uniaxial tension, Fig. 1. The material is assumed to obey a J_2 theory of plasticity with the viscosity law (6) given by

$$\dot{\gamma} = \dot{\gamma}_0 \left(\frac{\sigma_e}{\sigma_0(\gamma)} - 1 \right)^m \tag{13}$$

where $\dot{\gamma}_0$ is a reference strain rate, σ_e the Mises effective stress, and σ_0 the flow stress. Rate independent behavior is recovered as the rate sensitivity exponent $m \to \infty$. The flow stress is assumed to be a quadratic function of the effective plastic strain γ chosen such that, following an initial hardening stage, the material strain softens thereafter.

Fig. 2 shows the response of the element for several rate sensitivity exponents. Also shown for comparison are the results obtained from Hughes' $\bar{\mathbf{B}}$ isoparametric element (Hughes, 1980). The $\bar{\mathbf{B}}$ method is adopted here to avoid locking due to the near incompressibility of the element in the fully developed plastic flow regime. Every few steps after yielding, a linear perturbation analysis of the type outlined in Section 2 is conducted at the centroid of the element to detect the inception of localization and the geometry of the emerging localized modes. Once localization is detected, the strain interpolation of the element is enriched in the manner described in Section 3.

As the results shown in Fig. 2 indicate, for the nearly rate independent solid, corresponding to a value $m = 500$, localization occurs right at maximum load. As the rate sensitivity of the solid is raised, localization is delayed increasingly farther into the softening range. It is seen from Fig. 2 that the $\bar{\mathrm{B}}$ element is insensitive to localization and reproduces the uniform deformation solution. By contrast, the enhanced element exhibits the expected sharp drop in the force-displacement curve following the onset of localization. This result illustrates the need for specialized elements capable of adapting to the abruptly changing conditions characteristic of localization phenomena.

Next, we turn our attention to the dynamic response of frictional solids. The constitutive description adopted in the calculations is of the Drucker-Prager type (Drucker and Prager, 1952). A hardening law is introduced whereby the friction angle increases steadily with the accumulated effective plastic strain up to a saturation level, remaining constant thereafter. The dilatancy angle is taken to vanish throughout the analysis, which renders the plastic response non-associated. A detailed description of the constitutive model is given by Leroy and Ortiz (1989a, 1989b).

We consider a rectangular sample of the material constrained to undergo plane strain. The specimen is subjected to a prescribed velocity on its upper surface following a ramp variation in time. The specimen is supported on its lower surface. The impact velocity is 1/1200 of the elastic longitudinal wave speed. The time integration is carried out explicitly at roughly the elastic Courant stability limit. The rise time for the velocity is taken to be two time steps. An imperfection is introduced at the center of the specimen in the form of a slightly weaker element. Owing to the symmetries of the problem, the domain of the analysis is restricted to one quarter of the specimen.

Fig. 3 shows force-displacement curves for the rate independent solid obtained with two different mesh sizes. The quasi-static and uniform solutions are also shown for comparison. The circle on the dotted curve marks the critical bifurcation load under uniform deformation. The quasi-static force-displacement curve exhibits a sharp drop following localization, despite the fact that the material hardens at all times.

The dynamic response of the specimen ostensibly coincides for the two mesh sizes up to localization. As is evident from Fig. 3, the effect of localization on the force-displacement response of the specimen appears to be retarded by inertia. Well into the localized regime, the discrepancies between the results of the two meshes becomes more apparent, the coarser mesh delaying somewhat the progression of structural softening relative to the finer mesh.

The most striking differences between the quasi-static and the dynamic solutions concern the geometry of the shear bands. Whereas under quasi-static loading a single shear band emerges in each quarter of the specimen (Leroy and Ortiz, 1989a), a network of bands is seen to arise under dynamic conditions. Shown in Fig. 4 are the localized elements and localization directions for the finer mesh. The distribution of localized elements determines the location of the shear band. Again, the results are sensitive to mesh size variations, in that coarser meshes result in less intricate shear band patterns. Contours of effective plastic strain for the fine mesh are shown in Fig. 5. As may be seen, most of the deformation takes place along the primary shear band, the other branches playing a secondary role.

Finally, in order to assess the combined role of rate sensitivity and inertia as regards localization instabilities, the foregoing calculation is repeated for a linear overstress model. Details of the constitutive formulation may be found in the article of Leroy and Ortiz (1989b). Fig. 6 shows a comparison between the force-displacement curves for the dynamic rate dependent, dynamic rate independent and quasi-static rate dependent solutions. Also shown for reference is the uniform strain solution. Interestingly, the effect of rate dependence is seen to be rather minor up to localization. By contrast, following localization, a substantial delay in the structural softening is introduced by the rate dependence.

Contours of effective plastic strain for the rate dependent dynamic solution are shown in Fig. 7. Evidently, an effect of rate dependence is to broaden the shear band relative to the rate independent

solution. This effect is particularly manifest as one moves away from the nucleating defect and into the free surface. The activity within the secondary bands is also delayed by rate dependence relative to the rate independent solution, Fig. 7.

5. Discussion.

A noteworthy outcome of the computations reported here is the fact that the geometry of shear bands, both as regards their thickness and spatial distribution, is quite sensitive to rate dependence and inertia effects. There is also a strong influence of the geometry of the specimen and the presence of free boundaries. For instance, rate sensitivity appears to broaden the thickness of the band, which becomes a function of time. Under these conditions, the thickness is also nonuniform along the band, being broader away from stress concentration and close to free boundaries. In addition, inertia effects have been found to promote multiple shear banding, particularly at high impact velocities.

In view of these results, the prospects for describing the thickness of shear bands by means of a single material parameter, a feature common to many nonlocal and generalized continuum theories, do not seem particularly promising. At the very least, it appears that any such material parameter should be made a function of time, and allowed to depend on the rate of loading and on inertia in ways which are not fully understood at present.

Acknowledgement Support from the Office of Naval Research under grant $N00014-85-K-0720$ is gratefully acknowledged.

References

Aifantis, E.C., 1987, *Int. J. Plasticity*, 3, pp. 211-247.
Bazant, Z.P., and Pijaudier-Cabot, G., 1988, *J. Appl. Mech.*, 55, pp. 287-293.
Belytschko, T., Fish, J., and Engelmann, B.E., 1988, *Comp. Meth. Appl. Mech. Engr.*, 70, pp. 59-90.
de Borst, R., 1988, *Int. J. Num. Anal. Meth. Geomech.*, 12, pp. 99-17.
Chang, Y.W., and Asaro, R.J., 1981, *Acta Metall.*, 29, pp. 241-257.
Drucker, D.C., and Prager, W., 1952, *Q. J. Appl. Math.*, 10, pp. 157-165.
Frantziskonis, G., and Desai, C.S., 1987, *Int. J. Solids Structures*, 23, pp. 733-750.
Frantziskonis, G., and Desai, C.S., 1987, *Int. J. Solids Structures*, 23, pp. 751-767.
Freund, L.B., Wu, F.H., and Toulios, M., 1985, *Proc. Considère Memorial Symposium*, Ed. J. Salençon, Ecole Nationale des Ponts et Chaussées, Paris, 1985, pp. 125-134.
Hadamard, J., 1903, *Leçons sur la Propagation des Ondes et les Equations de L'Hydrodynamique*, Hermann, Chp. 6.
Hill, R., 1958, *J. Mech. Phys. Solids*, 6, pp. 236-249.
Hill, R., 1962, *J. Mech. Phys. Solids*, 10, pp. 1-16,
Hughes, T.J.R., 1980, *Int J. Num. Meth. Engr.*, 15, pp. 1413-1418.
Hutchinson, J.W., and Tvergaard, V., 1981, *Int. J. Solids Structures*, 17, pp. 451-470.
Leroy, Y., Needleman, A., and Ortiz, M., 1988, Preprint, *France - US Workshop on Strain Localization and Size Effect Due to Cracking and Damage*, Paris- Cachan, Sept. 1988.
Leroy, Y., and Ortiz, M., 1989a, *Int. J. Num. Anal. Meth. Geomech.*, 13, pp. 53-74.
Leroy, Y., and Ortiz, M., 1989b, *Int. J. Num. Anal. Meth. Geomech.*, (in press).
Molinari, A., and Clifton, R.J., 1987, *J. Appl. Mech.*, 54, pp. 806-812.
Molinari, A., 1987, *Proc. Int. CNRS Coll. on Nonlinear Phenomena in Materials Sciences*, Aussois, 1987.

Mandel, J., 1964, *Proc. IUTAM Symp. Rheology Soil Mech.*, Springer, pp. 59-68.
Marchand, A., and Duffy, J., 1988, *J. Mech. Phys. Solids*, **36**, pp. 251-283.
Marciniak, Z., and Kuczyński, K., 1967, *Int. J. Mech. Sci.*, **9**, pp. 609-620.
van Mier, J.G.M., 1984, *Ph.D. Dissertation*, De Technische Hogeschool Eindhoven, The Netherlands.
Mühlhaus, H.B., and Vardoulakis, I., 1987, *Géotechnique*, **37**, pp. 271-283.
Nacar, A., Needleman, A., and Ortiz, M., 1989, *Comp. Meth. Appl. Mech. Engr.*, (in press).
Needleman, A., and Tvergaard, V., 1982, *Finite Elements - Special Problems in Solid Mechanics*, J.T. Oden, and G.F. Carey, **5**, pp. 95-267.
Needleman, A. 1988, *Comp. Meth. Appl. Mech. Engr.*, **67**, pp. 69-85.
Needleman, A., 1989, *J. Appl. Mech.*, (in press).
Ortiz, M., Leroy, Y., and Needleman, A., 1987, *Comp. Meth. Appl. Mech. Engr.*, **61**, pp. 189-214.
Pijaudier-Cabot, G., and Bazant, Z.P., 1987, *J. Engr. Mech. Div., ASCE*, **113**, pp. 1512-1533.
Rice, J.R., 1976, *Theoretical and Applied Mechanics*, W.T. Koiter (ed.), North-Holland, pp. 207-220.
Rudnicki, J.W., and Rice, J.R., 1975, *J. Mech. Phys. Solids*, **23**, pp. 371-394.
Schreyer, H.L., and Chen, Z., 1984, *Constitutive equations: Macro and Computational Aspects*, K.J. William (ed.), ASME, New York, 193-203.
Thomas, T.Y., 1961, *Plastic Flow and Fracture in Solids*, Academic Press.
Triantafyllidis, N., and Aifantis, E.C., 1986, *J. Elasticity*, **16**, pp. 225-237.
Tvergaard, V., Needleman, A., and Lo, K.K., 1981, *J. Mech. Phys. Solids*, **29**, pp. 115-142.
Tvergaard, V., 1982, *J. Mech. Phys. Solids*, **30**, pp. 399-425.
Vardoulakis, I., 1979, *Acta Mechanica*, **32**, pp. 35-54.
Waversik, W.R., and Brace, W.F., 1971, *Rock Mech.*, **3**, pp. 61-85.
Zbib, H.M., and Aifantis, E.C., 1988, *Script. Metall.*, **22**, pp. 703-708.

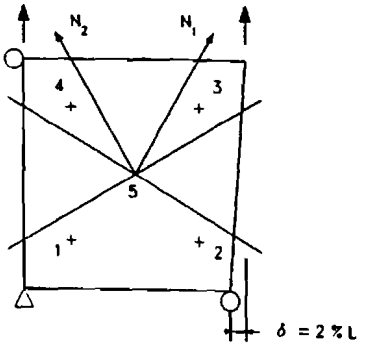

Fig. 1 One-element example.

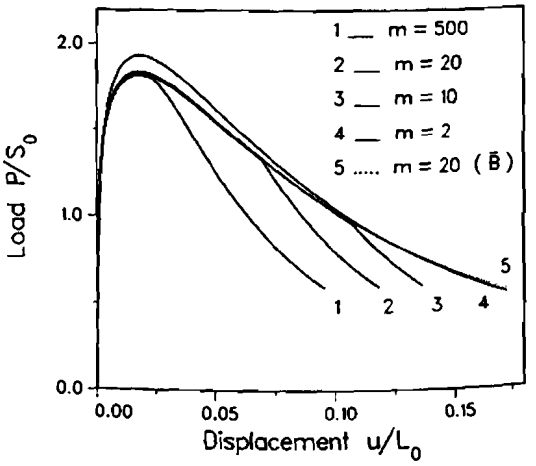

Fig. 2 Load-displacement curves for the one-element example.

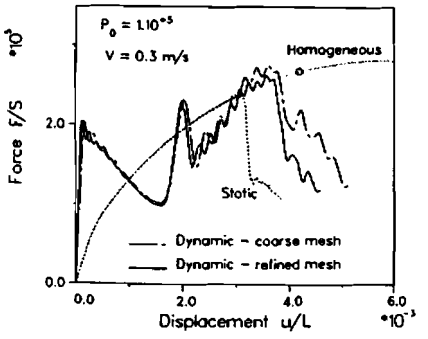

Fig. 3 Load-displacement curves for the rate independent tests.

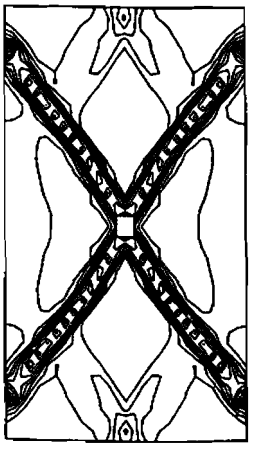

Fig. 5 Contours of effective plastic strain for the rate independent test (finer mesh).

Fig. 7 Contours of effective plastic strain for the rate dependent test.

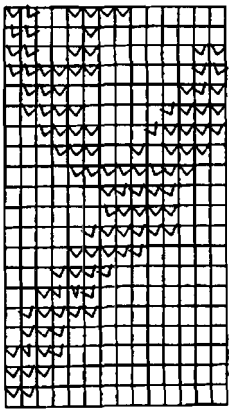

Fig. 4 Localized elements for the rate independent test (finer mesh).

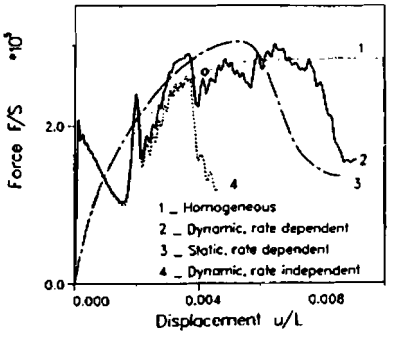

Fig. 6. Comparison of load-displacement curves.